JOURNAL OF NANO- AND ELECTRONIC PHYSICS
Vol. **10** No 5, 05029(4pp) (2018)

ЖУРНАЛ НАНО- ТА ЕЛЕКТРОННОЇ ФІЗИКИ
Том **10** № 5, 05029(4cc) (2018)

Optimize the Geometrical Parameters of Interdigital Micro-Electrodes Used in Bioimpedance Sensing System

Hamidreza Shirzadfar[1,*], Nasim Mokhtari[1], Julien Claudel[2]

[1] *Department of Biomedical Engineering, Sheikhbahaee University, Isfahan, Iran*
[2] *Institut Jean Lamour, CNRS, UMR 7198, Université de Lorraine, Vandœuvre-lès-Nancy, France*

(Received 17 July 2018; revised manuscript received 20 October 2018; published online 29 October 2018)

This paper is about optimizing the geometric parameters of the interdigitated electrodes. In this paper we optimize number of electrodes, length and width of them and the distance between them, in order to determine the electrical parameters such as relative permittivity and capacitance. The finite element method COMSOL Multiphysics® software in frequency range 10Hz to 1GHz is used in order to measure the electrical impedance of biological medium and simulate the particle separation in micro channel.

Keywords: Interdigital sensor, Biological medium, Optimization, Cell factor, Cut-off frequency, Particle separation

DOI: 10.21272/jnep.10(5).05029 PACS numbers: 87.85.fk, 85.85. + j

1. INTRODUCTION

Nowadays, there are enormous number of people are exposed to higher levels of diseases, disorders, infections, and pathogens [1]. The goal of this work is propose a new method to detect the abnormal red cells by using a new technology which permits to analyze the flow and blood solution. In this research, we use interdigital sensing device to evaluate the impedance of red blood cells and diagnose thalassemia by using blood cells separation. The red blood cell, called erythrocyte, is the natural form of a disk that is concave on both sides. The average diameter is about 7-8 microns and its main function is to transfer hemoglobin. Hemoglobin is a major component of the Red blood cells (RBCs) and a conjugated protein that carries respiratory gases [2]. The RBC consists of two types of protein, alpha and beta. If none of these proteins is sufficiently formed in the body, the red blood cells will lose their proper shape and cannot store the oxygen adequately. The result is anemia, which has been begun at early childhood and continues until the end of life. In thalassemia, the production of hemoglobin polypeptide chains is impaired and its synthesis is reduced and depending on the type of broken chain, thalassemia will be named.

Measuring the impedance of the biological tissues has been the interest of the researchers for more than a century and has been very effective in medical applications. The usage of the impedance spectroscopy, which is a useful and valuable method, shows the electrical response of a system to a time varying electrical excitation [3, 4]. This method of measuring the electrical impedance allows the physiological status of the body's tissues and even the electromagnetic properties of living tissues to be determined.

An ordinary interdigital electrodes array is a typical electrode configuration for the conductivity measurement applications [5]. One of the most important advantages of these sensors is the simple, miniature, and inexpensive production and manufacturing process [6]. In addition, is the ability to use them in a wide range of applications without significant changes in sensor design. Another potential benefit is the ability to integrate electrodes with instruments for the development of the independent measurement systems and labs on the chip.

2. THEORETICAL ANALYSIS AND OPTIMAZATION OF SENSOR

2.1 Equivalent Circuit Model of an Interdigital Sensor

The Fig. 1 represents the schematic of the sensor's structure. Each electrode has a width *W*, a length of electrodes *L* and a distance between two consecutive electrodes *S* [7-9]. This sensor is deposited on a thin glass substrate. When an electric voltage *U* between the two electrodes is applied, this voltage creates an electric field between each pair of electrodes (see Fig. 2).

This component is the sensitive measuring element. The R_{sol} is related to the conductivity of the medium σ and the cell factor K_{cell} depends entirely on the geometry of the sensor [10].

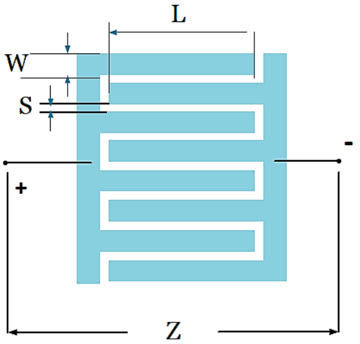

Fig. 1 – Schema of the geometric structure of an interdigital sensor

---

[*] h.shirzadfar@shbu.ac.ir
h.shirzadfar@gmail.com

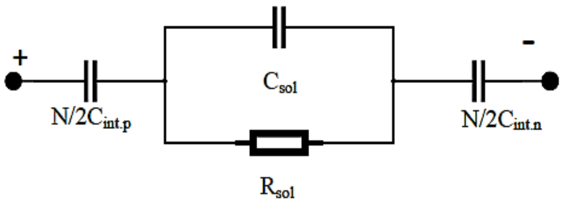

Fig. 2 – Simplified equivalent circuit model of interdigital sensor

2.2 Interface (Polarization) Impedance and Solution Impedance

The capacitance at the contact surface of each positive and negative electrode with the biological medium is represented by the capacitance *$C_{int.p}$*; and *$C_{int.n}$*. if, C_0 is the capacitance per unit area (pF/µm^2) and A is the surface of each electrodes (µm^2); Since the number of negative electrodes and the number of positive electrodes are the same (N/2), Thus, the total capacitance at the contact surface is determined by [11]:

$$C_{\text{interface}} = \frac{N}{4} LWC_0. \tag{1}$$

The polarization appears at the contact surface between electrodes and solutions. The impedance of polarization is determined by [11]:

$$Z_p = \frac{1}{j\omega C_{\text{interface}}}. \tag{2}$$

The impedance and the admittance are described by the following expressions [11]:

$$Z = \frac{K_{cell}}{\sigma + j\omega\varepsilon_0\varepsilon_r} \Rightarrow y = G + j\omega c = \frac{\sigma + j\omega\varepsilon_0\varepsilon_r}{K_{cell}}$$

$$\Rightarrow \begin{cases} G = \dfrac{\sigma}{K_{cell}} \\ C = \dfrac{\varepsilon_0\varepsilon_r}{K_{cell}} \end{cases} \tag{3}$$

where *j* is the imaginary symbol, *ω* is the angular pulsation (rad/s), *Z* is the complex impedance (*Ω*), Y is the complex admittance (*S*), *G* is the conductance (*S*), *C* is the capacitance (*F*). On the other hand, the total impedance and the total admittance in the equivalent electric circuit are calculated by [11]:

$$Z = \frac{1}{G_{sol} + j\omega C_{sol}} + \frac{1}{j\omega C_{\text{interface}}}. \tag{4}$$

The capacitance *C* can be determined as presented below [11]:

$$\Rightarrow \begin{cases} G = \dfrac{\omega^2 G_{sol} C_{\text{interface}}^2}{G_{sol}^2 + \omega^2 (C_{sol} + C_{\text{interface}})^2} \\ C = \dfrac{C_{\text{interface}} G_{sol}^2 + \omega^2 C_{sol} C_{\text{interface}} (C_{sol} + C_{\text{interface}})}{G_{sol}^2 + \omega^2 (C_{sol} + C_{\text{interface}})^2} \end{cases}, \tag{5}$$

where *ω* is approximately zero, the value of the total capacitance (*C*) equal to $C_{\text{interface}}$.

2.3 The Cut-Off Frequency

The main objective of this work is the geometrical optimization of the sensor structure in the cut-off frequency [11]:

$$f_{cut.off} = \frac{1}{2.\pi.R_{sol} C_{\text{interface}}}. \tag{6}$$

The equation of cut-off frequency (6) is thus rewritten as [3]:

$$f_{cut-low} = \frac{\sigma}{\pi.C_0} . \frac{N-1}{L.a} . \frac{K(\sqrt{1-k^2})}{K(k)}. \tag{7}$$

2.4 The Geometry Optimization of Electrodes

2.4.1 Optimization the Length of Electrode L

The Fig. 3 presents the cut-off frequency as a function of the length of electrodes L which calculated and obtained from formula (7). The parameters of this simulation is corresponding with the number of electrode which equal to $N = 40$ and the value of the metallization ratio $\alpha = 0.6$. we can realize that variation of cut-off frequency was strongly decreased when $L = 2000$ µm; and when $L = 2000$ µm the cut-off frequency variations are almost negligible.

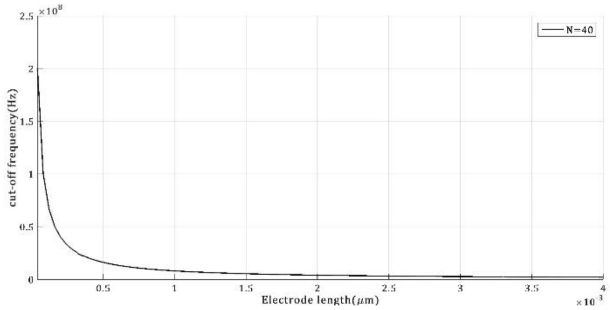

Fig. 3 – The result of cut-off frequency as a function of the length of electrodes *L* for optimization of $\alpha = 0.6$

2.4.2 Optimization of the Metallization Ratio a

From the formula (7), the relation between the cut-off frequency and the metallization ratio α is presented in Fig. 3. The cut-off frequency of the sensor passes through a minimum for $\alpha = 0.6$ corresponding to the sensor with $N = 40$ electrodes.

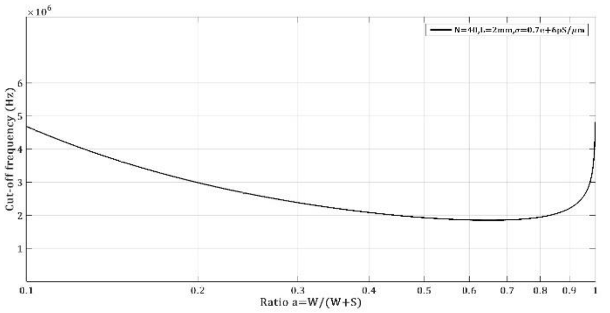

Fig. 4 – Cut-off frequency of the sensor as a function of the metallization ratio *α*

2.4.3 Optimization of the Electrode Number N

In addition, the optimal number of electrodes can be minimum equal to $N = 2$ which is the lowest possible number of electrodes. Thus, the modeling allows us to study the influence of electrode number N on the cell factor K_{cell}.

In Fig. 5, we observe a large variation in the cell factor of N in the range from 2 until 40 electrodes. In following, the variations in the cell factor are very weak for $N = 40$. Thus, we can choose $N = 40$ as a theoretical optimization of interdigitated electrodes. The parameters to optimize the sensor according different number of electrodes are calculated and indicated in Tabl. 1.

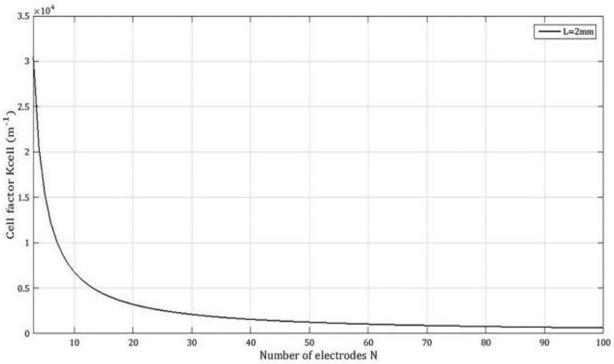

Fig. 5 – The result of the cell factor K_{cell} as a function of electrode number N

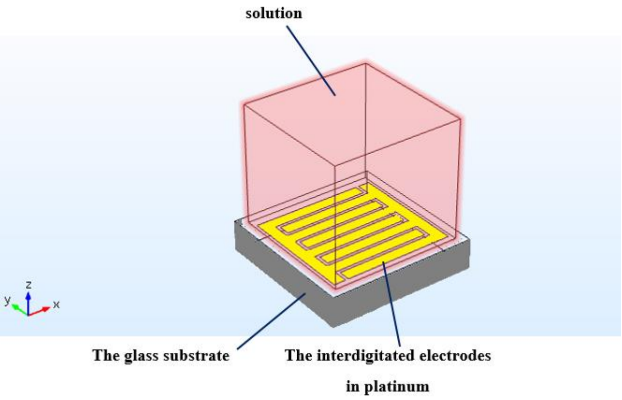

Fig. 6 – The 3D view model of electrodes type planar interdigitated electrode and it loaded by the full biological medium

3. MODELIZATION OF INTERDIGITATED SENSOR BY COMSOL MULTIPHYSICS

We have utilized the Comsol Multiphysics software to verify the theoretical results which achieved in previous section. This simulation permits to evaluate the influence of geometrical parameters of the interdigitated structure of the sensor and the dielectric properties of the medium [6]. The main objective of this simulation is to determine the impedance of blood samples.

Table 1 – The parameters of Interdigital sensor

Sensor	L(mm)	N	W(μm)	S(μm)	A	K_{cell} (m^{-1})	C_0 (PF/μm2)	$\varepsilon_{r,DL}$	D_{DL}(μm)
1	2	20	60	40	0.6	44.74	$1.7\cdot10^{-3}$	197.44	1
2	2	30	40	26.667	0.6	29.3121	$2.7\cdot10^{-3}$	301.35	1
3	2	40	30	20	0.6	21. 8	$3.6\cdot10^{-3}$	405	1
4	2	50	24	16	0.6	17.35	$4.5\cdot10^{-3}$	509	1
5	2	40	15	35	0.3	35.8	$4.7\cdot10^{-3}$	493.5	1
6	2	40	40	10	0.8	15.1	$3.9\cdot10^{-3}$	438.74	1

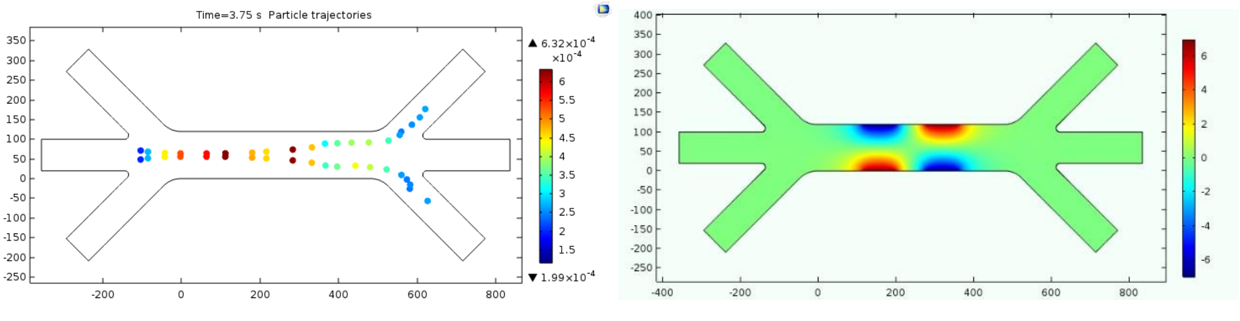

a b

Fig. 7 – The simulation results: (a) particle separation after passing from interdigitated electrode, (b) the distribution of electrical potential around the interdigitated sensor

3.1 Modeling of Interdigitated Sensor

The Fig. 6 shows the schematic of electrode sensors and sample that putted on the electrodes. The achieved results which simulated by Comsol are presented in Fig. 7a and b. The channel's shape is of glass because it is a good electrical insulator and we consider electrodes of platinum because of the best electrical conductivity ($9.42\cdot10^6$ Sm^{-1}) [12]. In this model, we first pass the solution with specific particles which the size of each particles are corresponding with the red cells and other blood's components through the micro channel. Then, by passing the tested medium away from the interdigitated electrodes and applying the dielectrophoresis force on it, the particle separation was carried out according to their diameter. This permits us to compare each particles with the reference results and for example it can be interesting and helpful to diagnose thalassemia by comparison the normal and abnormal red cells.

4. CONCLUSION

This paper presents a physical model of the interdigital sensor in the frequency range of 10 Hz to 1 GHz and we have proposed a new method to theoretically determine the parameters (relative permittivity, thickness and capacitance per unit area) of the double layer at the surface contact between the electrodes and the biological samples. Furthermore, the optimization calculations are done and theoretical calculations approach for optimizing the use of sensors for biochemical impedance spectroscopy.

The results of analytical simulations show the advantage of optimizing the components of the sensor. Finally, in this research, we have described the thalassemia disorder that was used to diagnose deformed blood cells by simulation in COMSOL Multiphysics® software. The 3D simulation techniques were used to analyze the effect of physical properties of the medium and impedance response by optimization the sensor's parameters. These results were defined theoretically in the first part and checked by simulation software. The theoretical and simulation results are in good agreement with idea to separate each particle and also study the characterization of any sample. In next step, we try to fabricate our sensor according to the optimization results and will prepare it to diagnostic blood's particles.

REFERENCES

1. H. Shirzadfar, M. Nadi, D. Kourtiche, S. Yamada, T. Hauet, *IRBM* **36** No 3, 178 (2015).
2. A.C. Guyton, J.E. Hall, J. Edward, *Texbook of Medical Physiology* (Elsivier: 2011).
3. S. Grimnes, OG. Martinsen. *Bioimpedance and Bioelectricity Basics* (Academic Press: 2000).
4. J. Claudel, M. Ibrahim, H. Shirzadfar, M. Nadi, O. Elmazria, D. Kourtiche. *XIII Mediterranean Conference on Medical and Biological Engineering and Computing 2013,* 841 (2014).
5. N.F Sheppard, R.C. Tucker, C. Wu. *Anal. Chem.* **65** No 9, 1199 (1993).
6. M. Ibrahim, J. Claudel, D. Kourtiche, M. Nadi, *J. Electr. Bioimpedance* **4**, 13 (2013).
7. R. Igreja, C.J. Dias, *Sensor. Actuat. A: Phys.* **112**, 291 (2004).
8. N.J. Kidner, Z.J. Homrighaus, T.O. Mason, E.J. Garboczi, *Thin Solid Films* **496**, 539 (2006).
9. C. Jungreuthmayer, G.M. Birnbaumer, P. Ertl, J. Zanghellini, *Sensor. Actuat. B: Chem.* **162**, 418 (2012).
10. T.T. Ngo, A. Bourjilat, J. Cloudel, D. Kourtiche, M. Nadi, *Next Gen. Sens. Syst.* 23 (2016).
11. T. Tuan Ngo, H. Shirzadfar, D. Kourtiche, M. Nadi, *J. Nano- Electron. Phys.* **6**, 01011 (2014).
12. T.T. Ngo, H. Shirzadfar, A. Bourjilat, D. Kourtiche, M. Nadi, *Proceedings of the 8th International Conference on Sensing Technology*, 348 (2014).